NASA Technical Memorandum 105551

X-Ray Based Displacement Measurement for Hostile Environments

Howard A. Canistraro, Eric H. Jordon, and Douglas M. Pease
University of Connecticut
Storrs, Connecticut

and

Gustave C. Fralick
Lewis Research Center
Cleveland, Ohio

March 1992

NASA

X-RAY BASED DISPLACEMENT MEASUREMENT FOR HOSTILE ENVIRONMENTS

Howard A. Canistraro, Eric H. Jordan, and Douglas M. Pease
University of Connecticut
Storrs, Connecticut 06268

and

Gustave C. Fralick
National Aeronautics and Space Administration
Lewis Research Center
Cleveland, Ohio 44135

SUMMARY

A completely new method of noncontacting, high-temperature extensometry based on the focus and scanning of x-rays is currently under development and shows great promise of overcoming many of the limitations associated with available techniques. The chief advantage is expected to be the ability to make undisturbed measurements through stratified or flowing gases, smoke and flame.

The system is based on the ability to focus and scan low energy, hard x-rays such as those emanating from copper or molybdenum sources. The x-rays are focused into a narrow and intense line image which can be scanned onto targets that fluoresce secondary x-ray radiation. This radiation is monitored and target edge position can be determined by measuring the beam pointing angle when the marker begins to fluoresce. The final goal of the system is the ability to conduct macroscopic strain measurement in hostile environments by utilizing two or more fluorescing targets. Current work has been limited to displacement measurement of a single target with a resolution of 1.25 μm and at target temperatures of 1200 °C, directly through an open flame. The main advantage of the technique lies in the penetrating nature of x-rays which are not affected by the presence of refracting gas layers, smoke, flame or intense thermal radiation, all of which could render conventional extensometry methods inoperative or greatly compromise their performance.

INTRODUCTION

Improved ability to produce engineering components for hostile environment use is very important for continued increases in efficiency of fuel burning engines, and is a prerequisite for successful development of the more ambitious hypersonic flight vehicles such as the National Aero Space Plane (NASP). A fundamental requirement of these and other advanced programs is the ability to measure the mechanical response of newly available materials under realistic operating conditions. These may include high-temperature - high-velocity gas flows, significant pressure gradients or the presence of flames and smoke. The measurement of strain and displacement under such conditions is very challenging and a limited number of available methods including high-temperature strain gages (ref. 1), ceramic rod extensometers (ref. 2), and laser optical systems (ref. 3) can be used under specific environmental conditions. Strain gages seem to be limited to temperatures below 1000 °C and strains of only a few thousand microstrain. Contacting extensometers present access problems in some cases and cannot be used in the presence of high-velocity gas flows. Laser based optical methods appear to be the least restrictive, but hot gases above ambient pressure are a severe problem because of refraction of the

source laser beam (ref. 4). In addition, smoke and dust can cause the accuracy of such systems to greatly deteriorate. The purpose of the present device is to provide a technique that can expand the range of conditions under which displacement and strain measurements can be performed.

BACKGROUND

During the course of the present work (ref. 5), examination of how to accomplish non-contacting displacement or strain measurement in the presence of refracting gas layers led to the consideration of employing electromagnetic radiation other than that of optical light; upon examination of longer wavelength radiation, it appeared that the infrared would experience worse interference effects from thermal radiation, and microwaves would probably experience limited resolution as a result of their long wavelength when compared to the required measurement accuracy. Investigation of shorter wavelengths revealed that the near ultraviolet was somewhat more refracting than optical light (ref. 6). For photon energies greater than this, however, one enters the vacuum ultraviolet (VUV) and soft x-ray regimes which require a vacuum for propagation (ref. 7). These factors led to the consideration of hard x-rays with the lowest possible energy, in order to minimize radiation hazard concerns. Hard x-rays are desirable considering their superior penetrating ability and low refractivity. The most commonly available sources of this kind are x-ray diffraction tubes employing either a copper filament with a characteristic radiation wavelength of 1.5 Å, or a molybdenum filament with a corresponding wavelength of 0.7 Å. In addition, this type of radiation is virtually unrefractable. For example, values of 1-n (n being the index of refraction) have been obtained by careful measurement of slight deviations from Bragg's law for copper source radiation reflected from mica, a metal-containing crystal. Deviations of n from unity are of the order 10^{-5} in this experiment (ref. 8). Thus, refraction in air or smoke would be nearly nonexistent. Both molybdenum and copper sources are now currently being used. Other types may be utilized in the future for specific applications.

The use of low energy, hard x-rays in strain measurement led to special problems associated with the inability to focus these rays in the conventional sense. There are no x-ray mirrors or lenses similar to those commonly associated with optical lasers. Instead, one is limited to line and point sources, and optics involving glancing angle reflection or Bragg governed reflection occurring on uniform crystal lattices. It was the latter method that was chosen due to the availability of ground and bent crystals which can focus a relatively large area of source radiation into a narrow line.

Once this focused x-ray line was produced, it had to be translated while maintaining focus and stability. The basic idea involved mounting the bent crystal on an arm which could be rotated while simultaneously allowing for Bragg reflection conditions to be maintained. It seemed obvious that if the center of rotation of this arm was placed directly below the x-ray line source, geometrical considerations would allow Bragg conditions to be satisfied, providing that the error in glancing angle and focusing distance were small during rotation.

Given this intense, scannable x-ray line image, a special strategy was developed in order to accomplish useful displacement measurements. The primary concept was to translate the image and cause it to overlap targets affixed to specimens or components. Upon stimulation by the incident beam, these targets fluoresce secondary radiation as a result of absorption edge behavior (refs. 9 and 10) which can subsequently be detected through the use of x-ray monitoring devices

such as plastic scintillation detectors. By measuring this secondary rate and comparing it to beam pointing angle, target edge position relative to beam pointing angle can be determined. Any change in target edge position perpendicular to the incident beam will now be apparent in subsequent beam-target overlap scans, and precise values of this displacement can be determined by comparing beam pointing angle versus secondary radiation curves for each target position, respectively. Figure 1 shows a typical displacement measuring system using the fluorescing technique, and for conceptual illustration, figure 2 shows an ideal single target, scanned by the x-ray image at two positions, with curves comparing secondary radiation and beam image position. It should be noted that if the target referred to in figure 2 had been moved a known distance, the offset between the curves would establish a calibration factor for the given equipment configuration, relating beam pointing angle to target displacement. A simple variation on this basic system is to allow the beam to be masked by an opaque target, which is placed between the x-ray source and the detector. Now, as the beam is scanned off the target edge, it is allowed to pass directly into the detector resulting in substantially higher count rates and greater resolution.

FIRST ORDER APPROXIMATION OF THE QUANTUM MEASUREMENT LIMITS

The fundamental quantity being measured is the intensity of fluoresced radiation, which is minute enough that individual photon counting is required. The arrival of such photons is a random event and governed by Poisson statistics, and intensity measurements are therefore subject to statistical fluctuation often referred to as "shot noise." This fluctuation is proportional to the square root of the counts collected and this uncertainty leads directly to a subsequent uncertainty in measured displacement that is dependent on the given beam intensity and geometry. It should be noted that the exact focused image geometry obtained using a typical bent crystal is complicated and unique to the specific crystal used, and depends on such factors as rocking curves, mosaicing, source size and perfection of the crystal itself. Thus, it is not possible to create a general description of the beam geometry that is realistic. Instead, we are limited to quantum error estimates based on an idealized image and we choose to use the simplest possible focused image geometry; uniform intensity and rectangular shape. This simplification is reasonable for two reasons; first our experiments show that for the displacement range typical of strain measurement, the beam is reasonably uniform, and secondly, if the developed equations are to be applied in the sense of finite difference calculus, the derived expressions will be the correct ones for local regions of an actual image-target overlap scan. The expressions developed are in no way relied upon to actually make displacement measurements, but are instead useful in deciding how much improvement in resolution is possible for an actual focused image-target system. This analysis also helps quantify the tradeoff between count period at each point of an overlap scan and potential resolution.

When attempting to predict the potential quantum limit of resolution of a given focused image-target system, the apparent change in target position as it relates to Poisson fluctuation of the secondary rate is related to the net count rate at a given overlap, and the slope of the overlap curve itself. The following quantities will be relevant to the estimation of the quantum limit:

$$\begin{aligned} &\text{Number of Counts collected} = N \\ &\text{Poisson Fluctuation} = \sqrt{N} \\ &\text{Beam Width} = W \\ &\text{Off Target Noise Floor} = e \end{aligned} \tag{1}$$

The fluctuation of secondary radiation manifests itself as apparent positional noise according to the following relation:

$$\text{Positional Noise} = \sqrt{N}/(dN/dx) \tag{2}$$

where dN/dx is the slope of the overlap curve at the given image overlap position. For the idealized beam profile as shown in figure 3, the derivative in the above equation is again the slope of the overlap curve and can be written as:

$$\text{Slope} = dN/dx = (N - e)/W \tag{3}$$

This quantity is denoted as m. By substituting the above expression into equation (2), the following positional noise expression for the idealized system becomes:

$$\text{Positional Noise} = N/m = W/\sqrt{N}(1 - e/N) \tag{4}$$

It is now possible to use equation (2) with slopes and count values from actual image-target overlap scans, to determine quantum limits of resolution. The user can then operate using only the portion of the image-target overlap having the maximum potential resolution.

It is clear that it is desirable to have the highest possible counts collected from the most brilliant scanning beam. Also, accuracy can be improved by collecting photons as long as practical for a given image target overlap, thereby reducing the effect of Poisson fluctuations by increasing the valve of N and increasing the slope of the overlap curve. As a result, it is possible to select higher accuracy at the expense of frequency response or vice-versa. An illustration of the tradeoff between the predicted quantum limit of resolution and scan period as given by equation (2), as well as our current experimental data points, which represent multiple scans at the shown displacement increments, are shown in figure 4. It can be seen that we have not reached the quantum limit of resolution (0.1 μm for the copper-cobalt combination and 0.5 μm for the molybdenum-yttria), primarily due to beam instability stemming from the antiquated nature of our x-ray generation system. For displacement measurements, the target edge position is declared a particular secondary rate, and determined directly from the overlap curve.

SYSTEM DESCRIPTION

The major system components are a stable x-ray source, a focusing crystal, an appropriate arm or table for scanning of the focused line image, a fluorescing or opaque target, an appropriate secondary radiation detector, and a data acquisition and processing system. Each of these system elements will be described as they are presently implemented, along with possible improvements.

X-Ray Source

The current experimental setup utilizes a 500 W x-ray generation system dating back to the 1950's, consisting of a power supply and a diffraction type x-ray tube. Typically, each tube emits two strong characteristic frequencies of radiation, an alpha and a beta "line," and we have used both to focus line images and conduct displacement measurements. For sources, copper (8 KeV) and molybdenum (17 KeV) x-ray radiation have been employed. By comparison,

radiographic inspection of metal parts is often done with x-rays with energies to 500 keV, revealing that the photon energies associated with the present effort are dramatically less dangerous than those found in the industrial and medical industries. Our current tube brilliance is approximately 20 W/mm^2 with a line width of 1.0 mm, and suffers from substantial instability stemming from the type of generator in use (ripple of 5 percent or greater in the power supplied to the tube). It is this instability that has caused us to count photons for greater lengths of time in order to overcome this inherent effect. Today's modern x-ray units are lightweight, can produce brilliancies of 600 W/mm^2 and have power supplies that are 50 times as stable as the one currently in use. In addition, rotating anode sources can produce brilliancies of up to 2000 W/mm^2. By producing a substantially more intense focused line image, fluoresced secondary radiation levels will vastly increase, allowing for greater resolution and reduction in measurement times.

X-Ray Focusing System

The foundation of the focusing system is Bragg reflection on specific crystal lattices. Recall that for a single lattice orientation and spacing, Bragg reflection of incoming radiation will occur over a small range of incident angles given a specific wavelength of radiation. These parameters are related by Bragg's law:

$$\begin{aligned} &n\lambda = 2D \sin\theta \\ &n = \text{any integer} \\ &\lambda = \text{wavelength of source radiation} \\ &D = \text{lattice spacing} \\ &\theta = \text{incident angle} \end{aligned} \tag{5}$$

By taking this planar lattice and bending it into a specific curve, Bragg conditions can be achieved over a larger area. This concept is shown in figure 5 and results in a line image at a specific spatial location relative to the bent crystal. Our current work has employed Johannsen ground and bent crystals (ref. 11), which employ a spherical cut to the surface and have very good focusing ability, resulting in an extremely intense x-ray image. Other crystals are also available such as Johann (ref. 12), Debroglie (ref. 13), and elastically bent types (refs. 14 and 15). In addition, a wide variety of crystals are commercially available or can be constructed to meet various focusing specifications. Our current focusing crystal is a lithium fluoride, ground and bent Johanssen type, with dimensions of 25 by 25 mm. The plane of reflection is the (200) orientation and has a focal length of approximately 24 cm when used with either a copper or molybdenum source tube. Direct beam count rates for the copper alpha line have been measured at 10^7 photons/second with a beam width of 0.08 cm. The molybdenum line is somewhat narrower at 0.03 cm with a direct count rate of approximately 10^6 photons/second when used with our outdated x-ray power supply. Much narrower and more intense line images may be produced by more exotic crystals such as the elastically bent type.

Scanning System

In order to conduct these types of measurements, beam stability and focus are critical, as any fluctuation in intensity would be misinterpreted as displacement. Because the focusing crystal only reflects for one incident angle, it is necessary to carefully consider how the beam is to be scanned. This task was accomplished by rotating the crystal on an arm whose center is located directly below the x-ray line source as shown in figure 6. Testing of direct beam count rates revealed stability of better than 1 percent over a 1.25 cm linear range (approximated by an

arc). Figure 7 is a photograph of the focused line at several beam pointing angles. In addition, beam pointing angle is measured from the arm using a precision LVDT type transducer which has a resolution of 0.1 μm, which corresponds to a displacement resolution at the focused beam image of 2.0×10^{-6} rad (or approximately 0.2 μm). For calibration purposes, a similar LVDT was also used for moving the fluorescing target known distances.

Target Selection

In theory, the ideal target would be one that fluoresces vigorously upon stimulation by the focused x-ray line, can withstand high-temperature hostile environments and be attached to the surface under investigation. High-fluorescing efficiency has been achieved by selecting target materials that have an x-ray absorption edge at or slightly below the energy of the bombarding x-rays, and under this condition maximum fluorescence is expected. After examining the behavior of several candidate materials, two specific pairs of source radiation-target materials have been selected: cobalt stimulated by copper source radiation and yttria stimulated by molybdenum. The cobalt responded well to both the focussed alpha and beta lines (fluorescing energy of 6 KeV) of a copper source tube and this metal has good high-temperature properties. The yttria-molybdenum system also proved to work quite well especially when the ytrria (fluorescing energy of 14 KeV) was used in a pure "fabric" form. The subsequent fluorescence is also penetrating and nonrefracting allowing for detection.

The yttria-molybdenum combination is more desirable due to the greater penetrating ability of molybdenum source radiation as well as the ability to "flame spray" yttria stabilized materials such as zirconia (ref. 16) onto actual components. Such flame sprayed coatings are routinely used in jet engine hot section parts and can have melting temperatures in excess of 2000 °C. In addition, all these target materials must be fashioned with a smooth, straight edge perpendicular to the gage section under investigation. The target length for all experiments has been approximately 4 cm. Experiments involving the use of plastic or other relatively soft routers to dress a straight edge on the coating are now being conducted.

Secondary Radiation Detection

Because the intent of the method is to allow remote sensing of displacement or strain in a hostile environment, detection needs to be done at a distance. Locating the detector far from the source will accomplish this goal, but can introduce view factor losses which will greatly impair the maximum resolution of the technique. This problem has been overcome by using a large detector in conjunction with state-of-the-art counting electronics. The detector employs a large (50- by 50-cm) plastic scintillator which funnels light pulses emanating from photon arrivals into a photo-multiplier tube (PMT) whose output is given directly to a high-speed amplifier and self contained, computer controlled counting unit. This system has proved to be quite effective and comparison of the output of the detector as measured on a high-speed digital oscilloscope versus the output of the electronic counting system has revealed that we are counting nearly every photon received by the PMT.

Data Acquisition and Processing

The self contained photon counting unit can be remotely controlled by any computer and instructed to count for specified periods of time. This output is then transferred in the form of a single number corresponding to a given time interval. The output from the beam pointing angle transducer is also simultaneously input to the computer via a voltage-to-frequency converter coupled with a high-speed counter board. This method was desirable due to its lower cost when compared to analog-to-digital (A-D) converters, and has effectively up to a 64-bit count register, compared to 12 bits found in better A-D converters. Secondary count rate versus beam position can now be plotted, curve fit and compared to other curves generated by different target positions in order to make displacement or strain measurements. Mathematical curve fitting allows for smoothing of the data, resulting in more precise displacement measurements.

TEST PROCEDURE

In order to make displacement measurements using this type of technique, a curve plotting secondary radiation versus beam pointing angle must be constructed. In addition, it is desirable to make this curve as steep as possible thereby minimizing the transition length of the focused line width onto the target edge. In general, the intensity of radiation across the focused line is not constant, therefore a straight line is not achieved. By curve fitting an entire overlap scan, and using the equation for resolution (eq. (4)), the zone of maximum resolution can be found by differentiation with respect to beam location.

Currently, overlap curves are constructed point by point. The beam is caused to slightly overlap the target edge and radiation is counted for a finite length of time, depending upon the desired resolution. When sufficient counts are obtained, the pointing angle and total count value are stored and the line is scanned further onto the target. The process is repeated until an entire overlap curve has been produced. At this point, the curve is examined and curve fit, and the zone of maximum resolution is found. Figure 8 shows an actual overlap curve with the zone of maximum resolution identified by the straight line. Scans for various target positions are now conducted in this area in order to exploit the lower limit of resolution possible.

Realizing that only two points are required to construct a straight line, a minimum two point scan is required at each target location, provided the scan is conducted in the zone of maximum potential resolution. Typically, the focused line is caused to overlap in the steep transition zone and counts are taken for a specified period of time. The image is then scanned further onto the target, and again photons are counted with the two points establishing a line. For the current results, four points have been used to establish the overlap line for each target position. The target can then be moved and the two or four point scan repeated. If the target displacement was accurately measured using an independent transducer, the offset between these two curves can be used to establish a calibration factor, which directly corresponds to beam image displacement at the target location for the given experimental configuration. This eliminates the need to precisely measure the radii of both the crystal arm transducer and the target from the center of rotation of the arm. Only the target radius is needed. At this point, displacement measurements at the target are possible with the indicated resolution.

TEST RESULTS

In order to prove repeatability, the target position is measured at known increments with four different target positions typically being measured. If the curves are regularly spaced, a calibration factor for the given experimental setup is established. Presently, the following displacement measurements of a single target have been conducted with the resolution shown.

- Cobalt target-copper source, 2.5 μm at 1200 °C through an open flame (propane type). Scan period 10 sec/point - four points/target position.

- Yttria fabric target - molybdenum source, 1.25 μm at room temperature. Scan period 10 sec/point - four points/target position.

- Yttria stabilized zirconia - molybdenum source, 2.5 μm at room temperature. Scan period 10 sec/point - four points/target position.

- Steel masking target - copper source (opaque target method), 1.25 μm at room temperature. Scan period 3 sec/point - four points/target position.

The data was also curve fit using a second order polynomial. Figure 9 shows a four target position scan with four data points taken at each target position, of a cobalt target stimulated by a copper source at a target spacing increment of 1.25 μm. Figure 10 shows a second order curve fit of the four scans with the x-axis converted to target displacement in microns. Curve fitting of the data will be critical in permitting system automation, where the computer will determine offsets between subsequent target scans. Note that in both cases, the curve spacing is quite regular. Additional measurements of unknown target displacements were then conducted with an expected resolution of 1.25 μm. It should be noted that the target of yttria stabilized zirconia was an actual thermal barrier coating (TBC) panel used on gas turbine engines.

MACROSCOPIC STRAIN MEASUREMENT

Many applications are likely to be possible, provided some modifications are made to the existing system. The first of these would be the use of two crystals focused simultaneously from a single source (fig. 11). This would result in two focused lines that would be a fixed distance apart and move together during the course of a scan, provided both crystals moved together. The use of two fluorescing targets would demarcate a gage length and strain could be determined by measuring the displacement of each target. Additionally, by setting the focused x-ray images at a distance smaller than the gage length, individual target fluorescence would occur at different times allowing for demodulation of the secondary radiation coming from each target. This type of system would greatly reduce "dead time" of the focused line during scanning. Given our current results, a gage length of 50.8 mm (2 in.) would yield a resolution of 25 microstrain.

SUBSURFACE STRAIN MEASUREMENT

Subsurface strain could also be determined by prepositioning targets in the substrate of a material. This type of technique would be useful in composite materials whenever the matrix is

transparent to low energy radiation (i.e., polymers and carbon-carbon). The targets could then be placed near critical features such as fibers.

RIGID BODY MOTION CONCERNS

The method proposed is subject to rigid body effects typical of other line of sight techniques such as laser based optical systems (ref. 4). In-plane translation is not a problem, and out-of-plane motion will only be of concern if it is large enough to produce a change in apparent angular size of the gage length. The most serious problem is rigid body rotations which must be limited to a degree or two. In the future, it may be possible to use three targets to obtain rotation information and correct for these effects. In any case, this and similar methods can be successfully used in materials testing where the rotations and out-of-plane motion are known to be small.

CONCLUSION

The penetrating, nonrefracting nature of x-rays will allow the technique to be used in situations where competing methods such as laser interferometry become unworkable. The x-ray system will permit noncontacting strain measurement at high temperatures and pressures, on both laboratory specimens and "real world" components. In addition, the device may be used in the presence of matter such as smoke, dust or even cutting fluid, which would otherwise render conventional systems ineffective.

The application of x-ray based extensometry to programs such as the National Aerospace Plane (NASP), advanced high-temperature composites, and any other area where material behavior in the presence of hostile environments is a fundamental design parameter, appears possible.

ACKNOWLEDGMENTS

The authors wish to express their appreciation to Dr. Dan Williams of the NASA Lewis Research Center for his continued support (NASA grant NAG3-1004).

We would also like to thank John Fikiet and Dale Brewe for their significant contributions to the project.

REFERENCES

1. Wu, T.-T.; Ma, L.-C.; and Zhao, L.-B.: Development of Temperature—Compensated Strain Gages for Use up to 700 Degrees C. Exp. Mech., vol. 21, no. 3, Mar. 1981, pp. 117-123.

2. Hulse, R.S., et al.: High Temperature Static Strain Gage Development. NASA CR-189044, 1991.

3. Carroll, D.F.; and Wiederhorn, S.M.: A Technique for Tensile Creep Testing of Ceramics. Am. Ceram. Soc. J., vol. 72, no. 9, 1989, pp. 1610-1614.

4. Sharpe, W.N.; Payne, T.S.; and Smith, M.K.: Biaxial Laser Based Displacement Transducer. Rev. Sci. Instrum., vol. 49, no. 6, 1978, pp. 741-745.

5. Jordan, E.H., et al.: High Temperature Displacement Measurement Using A Scanning Focused X-Ray Line Source. Advances in X-Ray Analysis, C.S. Barrett, ed., Plenum Press, New York, 1991.

6. Halliday, D.; and Resnick, R.: Fundamentals of Physics. Second ed. Wiley, 1981.

7. Kunz, C.: Introduction—Properties of Synchrotron Radiation. Springer, 1979.

8. Richtmeyer, F.K.; Kennard, E.H.; and Lauritsen, T.: Introduction to Modern Physics. Fifth ed. McGraw-Hill, 1955.

9. Herglotz, H.K.; and Birks, L.S.: X-Ray Spectrometry. Marcel Dekker, Inc., 1978.

10. Compton, A.H.; and Allison, S.K.: X-Rays in Theory and Experiment. Van Nostrand, 1935.

11. Johansson, T.: Selective Focusing of X-Rays. Naturwiss., vol. 20, 1932, pp. 758-759.

12. Johann, H.H.: Intense X-Ray Spectra Obtained with Concave Crystals. Z. Physik., vol. 69, no. 3-4, May 1931, pp. 185-206.

13. DeBroglie, M.: and Lindemann, F.A.: A Method for Rapidly Obtaining Spectra of Rontgen Rays. Compt. Rend., vol. 158, 1914, pp. 994,945.

14. Suortti, P.; Pattison, P.; and Werrich, W.: An X-Ray Spectrometer for Inelastic Scattering Experiments: I. Curved Crystal Optics. J. Appl. Crystal., vol. 19, Oct. 1986, pp. 346-342.

15. Suortti, P.; Pattison, P.; and Werrich, W.: An X-Ray Spectrometer for Inelastic Scattering Experiments: II. Spectral Flux and Resolution. J. Appl. Crystal., vol. 19, Oct. 1986, pp. 343-352.

16. Meier, S.M.; Gupta, D.K.; and Sheffler, K.D.: Ceramic Thermal Barrier Coatings for Commercial Gas Turbine Engines. J. Met., vol. 43, no. 3, Mar. 1991, pp. 50-53.

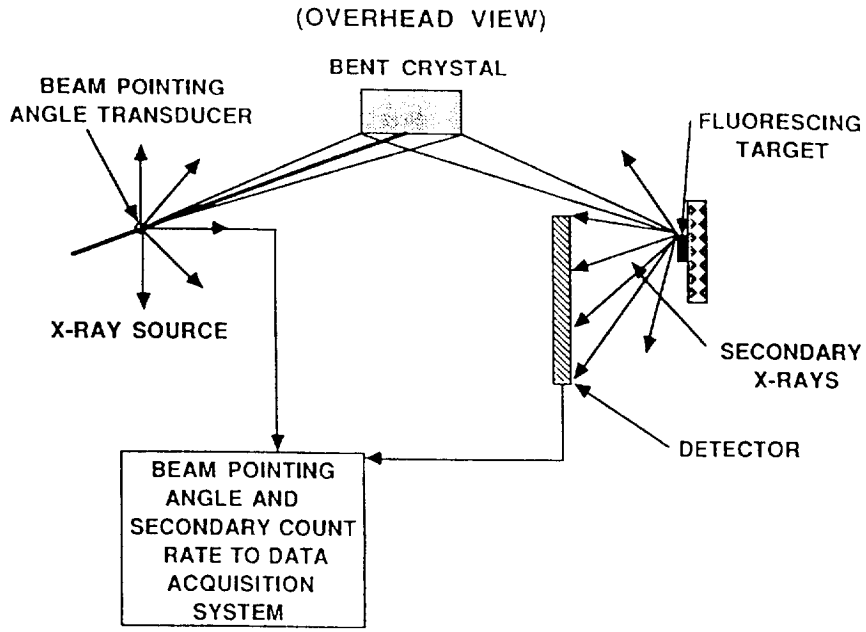

Figure 1.—Schematic view of a typical displacement measuring system.

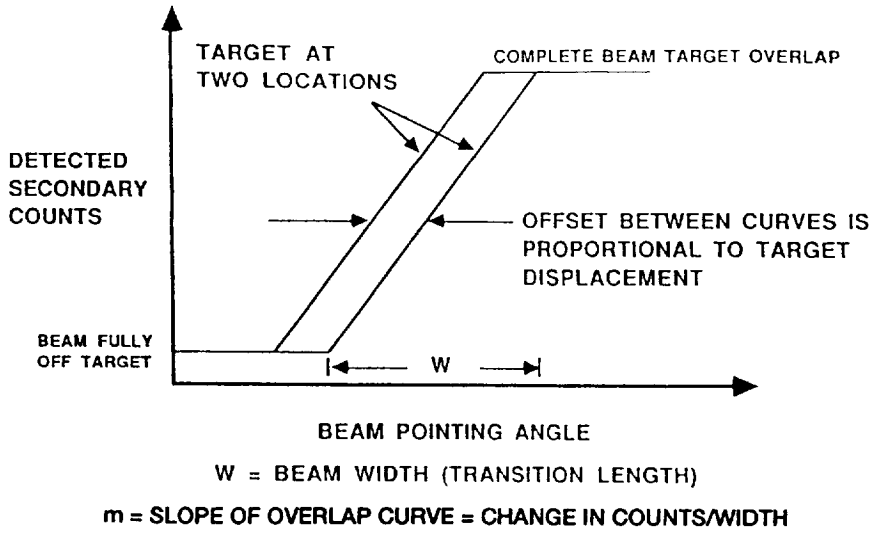

W = BEAM WIDTH (TRANSITION LENGTH)

m = SLOPE OF OVERLAP CURVE = CHANGE IN COUNTS/WIDTH

Figure 2.—A theoretical scan at two target positions. The offset between the two is proportional of target displacement.

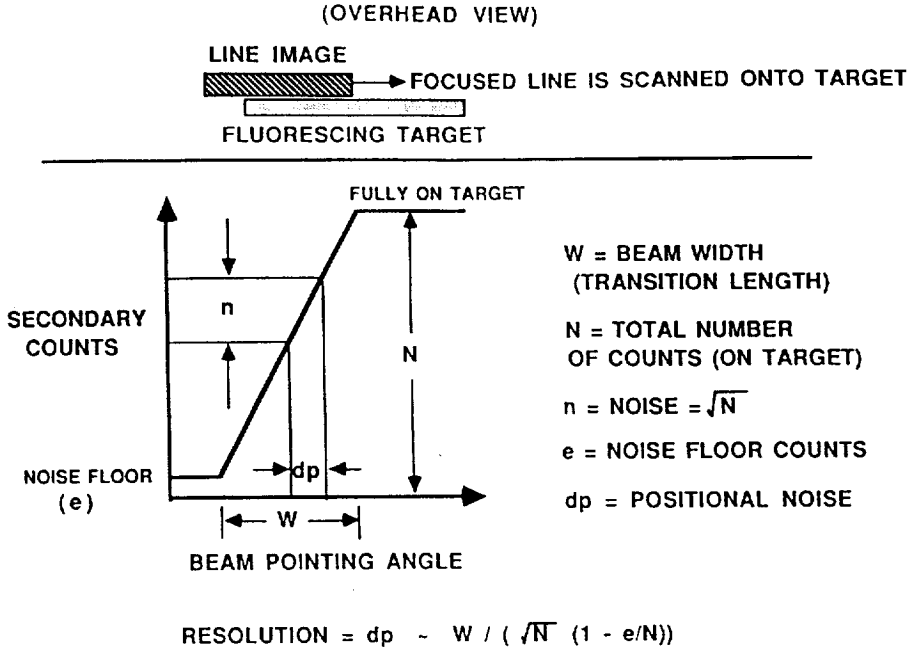

RESOLUTION = dp ~ W / ($\sqrt{N}$ (1 - e/N))

Figure 3.—An idealized overlap curve illustrating the relation between displacement resolution, countrate and slope of overlap curve.

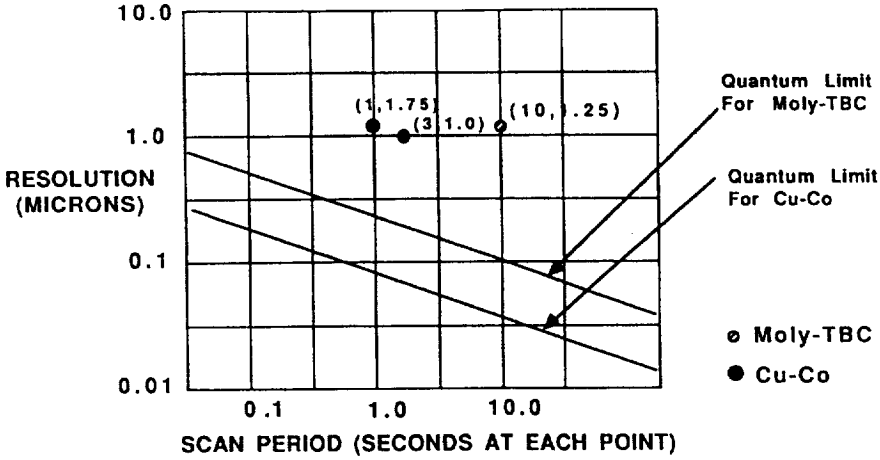

RESOLUTION ~ EFFECTIVE BEAM WIDTH/(COUNTRATE x PERIOD) $^{1/2}$

(Neglecting off target count noise)

*FOR GIVEN SECONDARY COUNT RATES AND OVERLAP SLOPES

Figure 4.—Shows the relation between scan time and resolution for various curve slopes and count rates. The longer the counting period, the greater the resolution possible, for a given level of flourescence and slope.

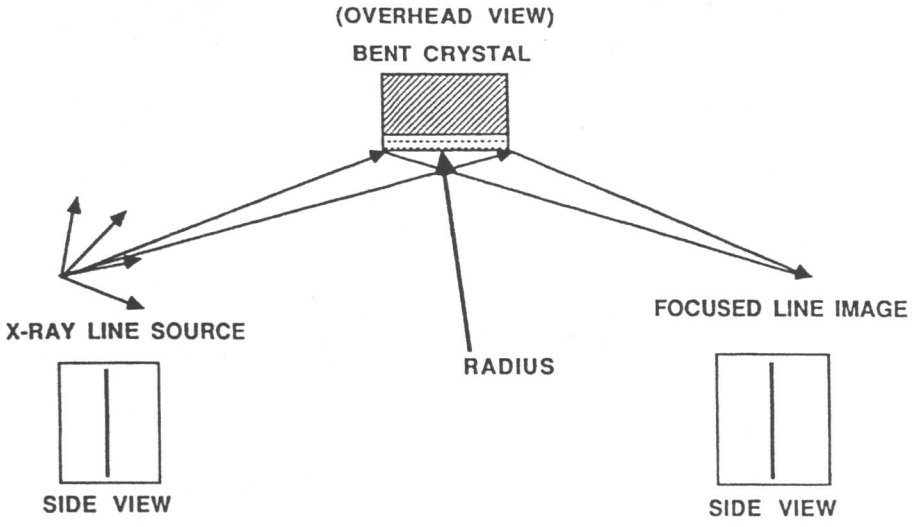

Figure 5.—Illustration of Bragg x-ray reflection from the surface of a typical ground and bent crystal.

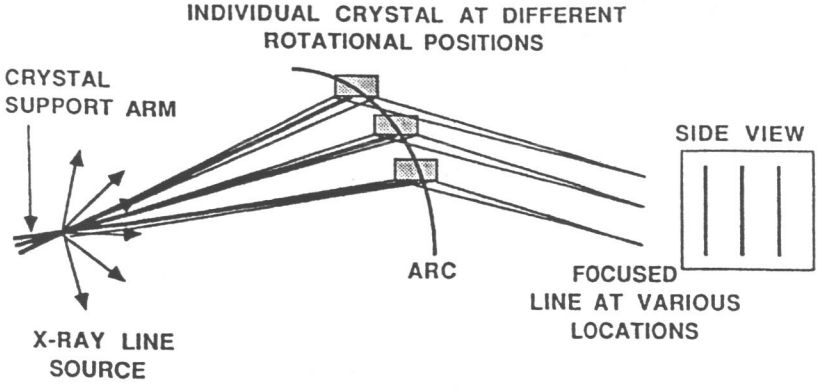

Figure 6.—Demonstration of focused line image scanning using a rotational arm.

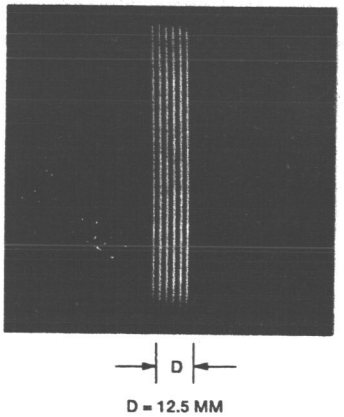

Figure 7.—Reproduction of a photograph of a focused line image at several beam pointing angles.

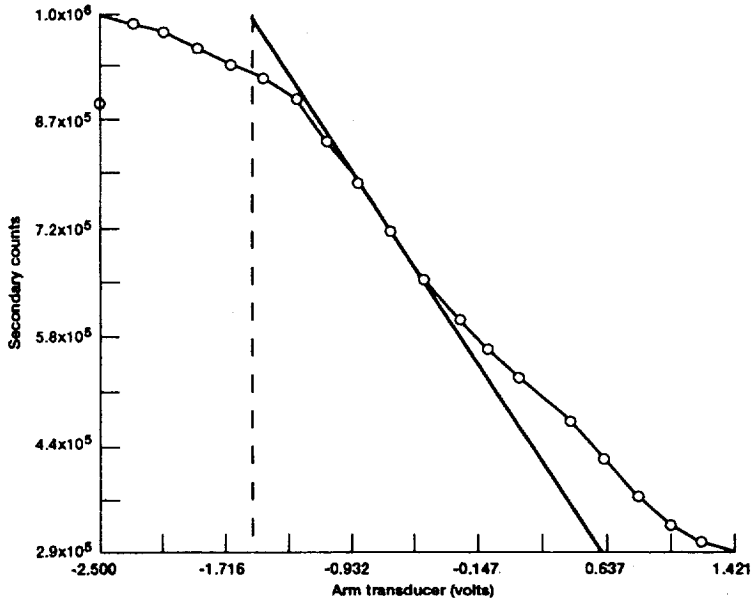

Figure 8.—Complete beam-target overlap curve for a yttria target stimulated by a molydenum target. There was a single scan over the entire transition length, with a 3 second count period at each point. Note steepest portion of overlap curve.

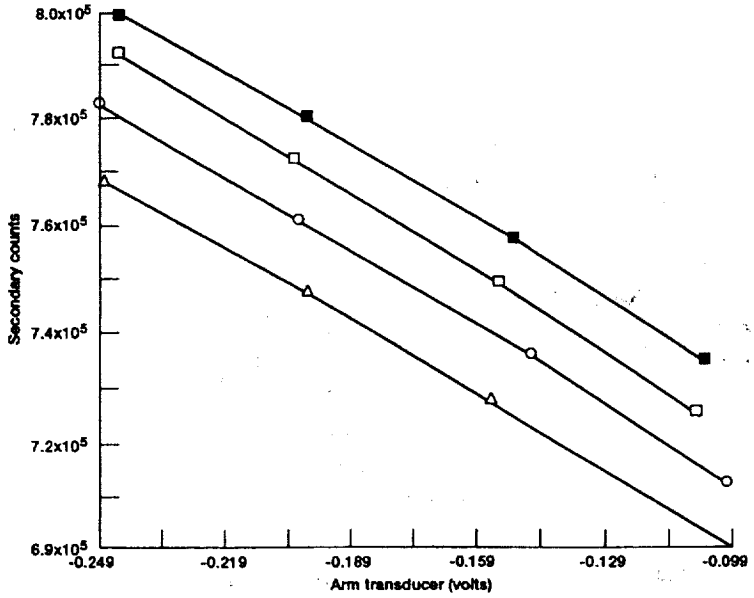

Figure 9.—Four scans, showing steepest portion of overlap curve for each. The spacing between curves corresponds to a 1.25 micron target displacement. A copper source was used, with a cobalt target. There was a 3 second count period at each point.

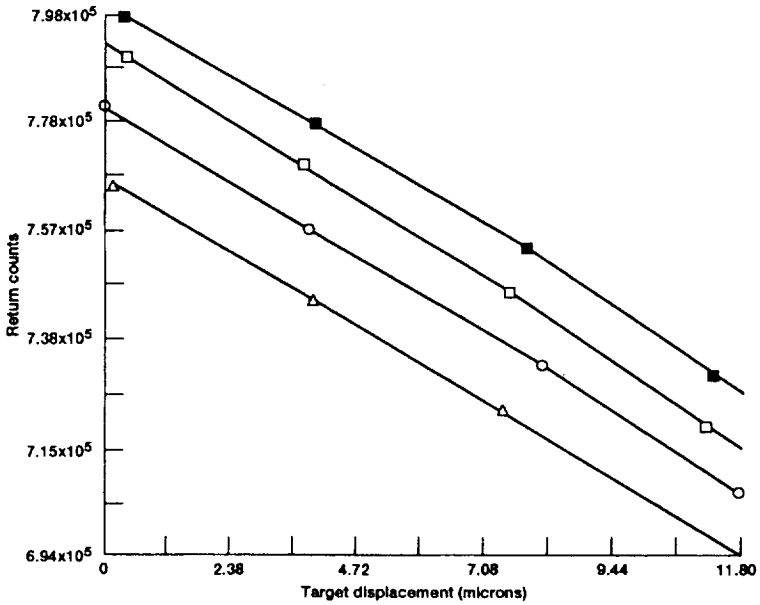

Figure 10.—A second order curve fit of the data in Fig. 9. Note that the x axis has been changed to reflect target displacements. These values were determined using a calibration factor derived graphically from the spacing between subsequent scans (0.01272 volts/micron).

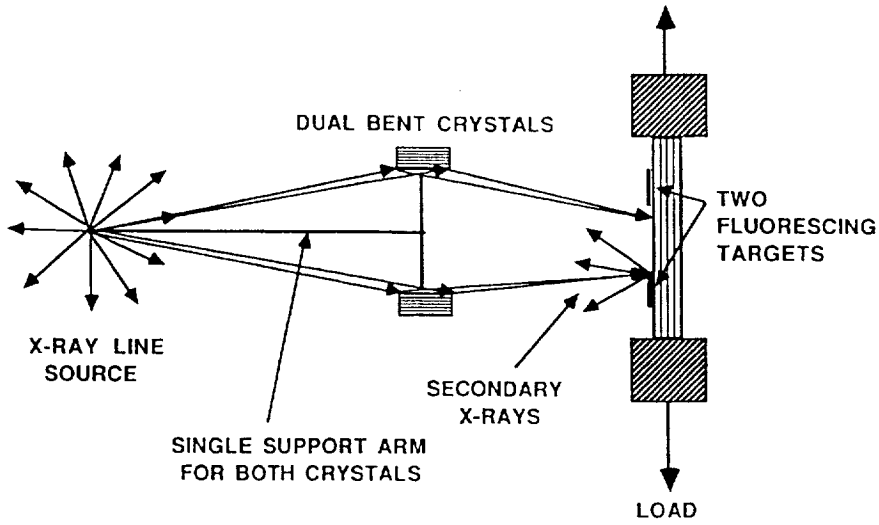

Figure 11.—Strain measurement system using two crystals simultaneously focusing two line images. The targets demarcate a gage length.

REPORT DOCUMENTATION PAGE

Form Approved
OMB No. 0704-0188

1. AGENCY USE ONLY (*Leave blank*)	2. REPORT DATE	3. REPORT TYPE AND DATES COVERED
	March 1992	Technical Memorandum

4. TITLE AND SUBTITLE

X-Ray Based Displacement Measurement for Hostile Environments

5. FUNDING NUMBERS

WU-505-90-01

6. AUTHOR(S)

Howard A. Canistraro, Eric H. Jordon, Douglas M. Pease, and
Gustave C. Fralick

7. PERFORMING ORGANIZATION NAME(S) AND ADDRESS(ES)

National Aeronautics and Space Administration
Lewis Research Center
Cleveland, Ohio 44135-3191

8. PERFORMING ORGANIZATION REPORT NUMBER

E-6872

9. SPONSORING/MONITORING AGENCY NAMES(S) AND ADDRESS(ES)

National Aeronautics and Space Administration
Washington, D.C. 20546-0001

10. SPONSORING/MONITORING AGENCY REPORT NUMBER

NASA TM-105551

11. SUPPLEMENTARY NOTES

Howard A. Canistraro, Eric H. Jordon, and Douglas M. Pease, University of Connecticut, Storrs, Connecticut, 06268 (work funded by NASA Grant NAG3-1004). Gustave C. Fralick, NASA Lewis Research Center. Responsible person Gustave C. Fralick, (216) 433-3645.

12a. DISTRIBUTION/AVAILABILITY STATEMENT

Unclassified - Unlimited
Subject Categories 35 and 39

12b. DISTRIBUTION CODE

13. ABSTRACT ***(Maximum 200 words)***

A completely new method of noncontacting, high-temperature extensometry based on the focus and scanning of x-rays is currently under development and shows promise of overcoming many of the limitations associated with available techniques. The chief advantage is expected to be the ability to make undisturbed measurements through stratified or flowing gases, smoke and flame. The system is based on the ability to focus and scan low energy, hard x-rays such as those emanating from copper or molybdenum sources. The x-rays are focused into a narrow and intense line image which can be scanned onto targets that fluoresce secondary x-ray radiation. This radiation is monitored and target edge position can be determined by measuring the beam pointing angle when the marker begins to fluoresce. The final goal of the system is the ability to conduct macroscopic strain measurement in hostile environments by utilizing two or more fluorescing targets. Current work has been limited to displacement measurement of a single target with a resolution of 1.25 micron and at target temperatures of 1200 degrees C, directly through an open flame. The main advantage of the technique lies in the penetrating nature of x-rays, which are not affected by the presence of refracting gas layers, smoke, flame or intense thermal radiation, all of which could render conventional extensometry methods inoperative or greatly compromise their performance.

14. SUBJECT TERMS	15. NUMBER OF PAGES
Strain; Extensometry; Non-contact; X-ray	16
	16. PRICE CODE: A03

17. SECURITY CLASSIFICATION OF REPORT	18. SECURITY CLASSIFICATION OF THIS PAGE	19. SECURITY CLASSIFICATION OF ABSTRACT	20. LIMITATION OF ABSTRACT
Unclassified	Unclassified	Unclassified	